

OPTIMIZATION OF WELDING PARAMETERS FOR GAS TRANSPORTATION STEEL PIPES

Received – Prispjelo: 2009-09-22
Accepted – Prihvaćeno: 2009-11-05
Preliminary Note – Prethodno priopćenje

The aim of this paper is to define optimization of welding conditions for Submerged Arc Welding (SAW) of steel pipes for gas transportation. Fine grain steel X-52 with thickness of 8 mm were used as a base material. Welding was performed from inner and outer side. Two wires, inclined under different angles, were feed separately. Eleven samples divided in three series were experimentally welded. Performed investigations indicated that the best properties showed weldments from series III, welded with the highest heat input. On the contrary of our expectations, welds from series II, using self made equipment, showed pretty bead properties and improper geometry. So, improving of this this equipment and obtaining welds with better properties is the target in future investigations.

Key words: welding parameters, microalloyed steel, tandem process

Optimizacija parametra zavarivanja čeličnih cijevi za plinovode. Cilj ovog rada je definirati optimizaciju parametara zavarivanja pod praškom čeličnih cijevi za plinovode. Finozrnati čelik X-52 debljine 8 mm je korišten kao osnovni materijal. Zavarivanje je izvedeno s vanjske i unutarnje strane. Dvije žice, pod različitim kutom su dodavane odvojeno. Jedanaest uzoraka, podijeljenih u tri serije eksperimentalno je zavareno. Ispitivanja su pokazala da najbolja svojstva imaju zavari iz serije III, zavareni s najvećom količinom unesene toplote. Suprotno očekivanjima, zavari iz serije II, kod kojih je korištena oprema koju su izradili autori rada, pokazali su vrlo lose karakteristike i neadekvatnu geometriju spoja. Stoga je osnovni cilj u sljedećim istraživanjima poboljšanje ove opreme u cilju dobijanja kvalitetnijih zavara.

Gljučne riječi: parametri zavarivanja, mikrolegirani čelik, zavarivanje s dvije žice

INTRODUCTION

Steel pipes still have the main roll in petrochemical industry. Submerged Arc Welding (SAW) process could be treated as one of the most important processes for obtaining longitudinally welded steel pipes, mainly due to the very good quality of welded joints and high productivity. However the defects in welded joints often lead to damage of installations and even more dangerous - human victims [1-3].

Therefore the optimization of welding parameters is the most important task in order to obtain welded pipes with high exploitation safety, which is also the main aim of the investigations presented in this paper.

SETUP OF EXPERIMENT

Steel plates of 8 mm thickness with designation X-52, were used as a base material for the production of welded pipes for gas transportation. Specification of steels for pipeline production, for petrochemical indus-

try is in accordance with American standard API 5L [4]. According to this standard, "X" represents longitudinally welded pipes, and "52" shows minimal tensile strength of 520 N/mm². Chemical composition and mechanical properties of the base material are given in Tables 1 and 2.

Prior to welding, plates of a base material were formed as pipe segments and tack welded using Shield Metal Arc Welding (SMAW) process with basic electrode, classified as E 42 4 B 32 H 5 according EN 499, (ϕ 3,25 mm). SAW welding process was performed us-

Table 1 **Chemical composition of base material for pipeline production, steel X52 [4]**

Chem. elem.	C	Si	Mn	P	S	Nb	Ti
Mas. %	0,059	0,27	0,9	0,007	0,013	0,023	0,01

Table 2 **Mechanical properties of base material in rolling (R) and transverse (T) directions, steel X52 [4]**

	R _e / N/mm ²	R _m / N/mm ²	A ₅ / %	KV / J -40 °C
R dir.	439	510	27,0	275, 301, 341, 305
T dir.	422	492	28,0	174, 170, 171, 171

S. Cvetkovski, D. Slavkov, Faculty of Technology and Metallurgy, Skopje, Republic of Macedonia; V. Grabulov, Z. Odanovic, Institute for materials testing, Republic of Serbia

Table 3 Chemical composition of weld metal (L-70 wire) [4, 5]

Ch. elem.	C	Mn	Si _{max}
Mass. %	0,109	0,91	0,14
Mo _{max}	Cu _{max}	S _{max}	P _{max}
0,5	0,77	0,009	0,007

ing welding wire L-70 ($\phi 4$ mm) with chemical composition given in Table 3 [4, 5]. The welding wire has the following mechanical properties: $R_e = 400$ N/mm², $R_m = 520$ N/mm², $A_5 = 25$ % and $KV = 133$ J at -40 °C.

The welding wire L-70 is generally used in order to satisfy the high toughness requirement of welding joints. Neutral welding flux Lincoln 995 (granulation: 0,2-2,5 mm) was used for single layer butt welding. The flux can be used five times in welding process, and it is recommended to perform draying at temperature of 300 °C/2h before welding [5]. Welding was conducted at the both sides of the pipe, with two wires for each run, which is known as tandem process. The first wire was connected to direct current (DC, + pole) and the second wire to the alternating current (AC). There was no gap between the edges of the pipes. Experimental welding of the steel pipes was performed for 11 samples, welded on automatic SAW machines ELLIRA [6]. One machine was used for inner and other for outer welding, while the maximum current for the both machines was 1200 A. The first weld was performed from inner side and was made under the same conditions for all segments.

Inclination of torches, distance between torches and tip of the wire (stick out) is shown in Figure 1.

The following parameters were used for this welding process: Wire I (welding current 460 A, welding voltage 26 V, welding speed 1,16 m/min) and Wire II (welding current 480 A, arc voltage 32 V and welding speed 1,16 m/min). Since the basic task in this investigation is to obtain optimal geometry of outer welds, three types of experiments (series) were performed.

Series I. Welding was performed under the conditions shown in Figure 2, with manual regulation of welding geometry along the weld length. Two segments 1 and 2 were welded in this way. Welding parameters which were used are given in Table 4. As can be seen

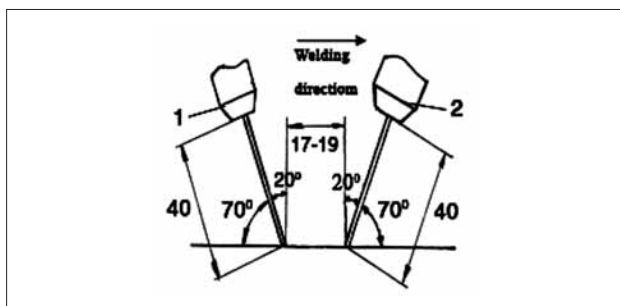


Figure 1 Welding geometry for inner tandem welding

Table 4 Welding parameter for segments 1 and 2 from Series I

Ser No	Weld. Param.	Segment 1		Segment 2	
		Wire I	Wire II	Wire I	Wire II
I	Current / A	460	480-500	510	520
	Arc voltage / V	26	28	30-32	36-38
	Weld speed / (m/min)	1,12	1,12	1,12	1,12

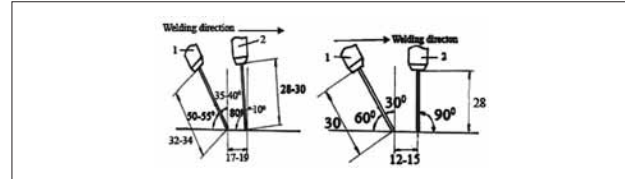


Figure 2 Welding geometry for series II, (left)

Figure 3 Welding geometry for series III, (right)

from the table 4, higher amperage and arc voltage were used for segment 2.

Series II. Welding was performed using self-made equipment which aimed to maintain the uniform geometry. Four segments with different geometry were welded using this approach. Segments 3 and 4 were welded as shown in Figure 2, while segments 5 and 6 were welded as shown in Figure 3.

Series III. Five segments (7-11) were welded under the conditions shown in Figure 3, with manual maintain of welding geometry. In order to obtain dipper penetration for this series, higher welding parameters were used. The torch angle for the first and second wire was 90° and 60°, respectively. Welding parameters for segment 7-11 are given in Table 6.

Macro, micro and fractographic analysis were performed to the welded joints produced in these investigations. Testing of the mechanical properties and hardness were also performed at the sample of the Serie III.

Table 5 Welding parameter for segments 3, 4, 5 and 6 from Series II

Ser No	Weld. Param.	Segment 3 and 4		Segment 5 and 6	
		Wire I	Wire II	Wire I	Wire II
II	Current / A	510	500-520	680	580
	Arc voltage. / V	30	36	30-32	40-42
	Weld speed / (m/min)	1,12	1,06	1,12	1,16

Table 6 Welding parameters for segment 7-11, Series III

Ser. No	Weld. Param.	Segment 7	
		Wire I	Wire II
III	Current / A	680	580
	Arc voltage. / V	32	40
	Weld speed / (m/min)	1,4	1,4

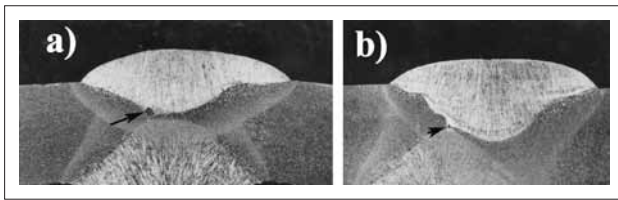


Figure 4 Macroscopic observation of segments 1 and 2 from series I weldments (a, b respectively), etched in Nital

ANALYSIS OF RESULTS

Macrostructure investigations of all welded joints were performed and the results for Series I to III are presented in Figures 4 to 6. Metallographic analyses of the Series I segments has shown low penetration between the welds, especially for the first segment (Figure 4a), because of the low current 460 A. In addition, misalignment between the welds was observed (the second segment, Figure 4b). Reinforcement of the faces were 1,8 - 2 mm for the first and 1,8 - 2,5 mm for the second segment. It is observed that weld shapes in both segments are not regular. The row of pores in both segments was observed by radiographic control. Pores can be seen on metallographic specimen in Figure 4 (arrows).

Macroscopic results of the Series II are presented in Figure 5. Rows of pores, insufficient root penetration and misalignment of welds are the defects which were found in all welded segments. In addition, it was shown that with this equipment and welding procedure this equipment was not able to completely maintain the uniform geometry. Higher penetration which can be seen in Figure 5 is a result of the fact that probes are taken at the beginning of the weld, when the geometry of welding is still irregular. Proper penetration between the welds is obtained in Serie (Figure 6), as a result of the higher welding parameter use. Dimensional, radiographic and metallographic control was conducted for each segment. Radiographic control showed small number of isolated pores in the welds. Weld penetration was recorded to be between 4,2 and 5 mm and all segments showed good welded joints characteristics. It was observed that the segment 7 in Figure 6a had the best characteristics. Welding speed during this process was 1,4 m/min. As can be seen from Figure 6b, segment 10 showed just little lower penetration.

Metallographic observations were conducted on segment 7, (Series III), in order to analyze microstructural characteristics of different areas in SAW joints. Figure 7 shows the locations of the microstructural observations. Microstructure of those areas of welded joint can be seen in Figure 8 (a-f).

Figure 8a show dendritic microstructure of weld metal. It was observed that the elongated dendrites propagate parallel with cooling direction. Traces of proeutectoid ferrite (PF) on the boundaries of primary

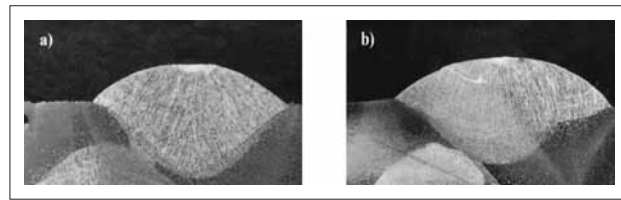


Figure 5 (a and b) Macro photos of series II weldments, segments 3 and 5, etched in Nital

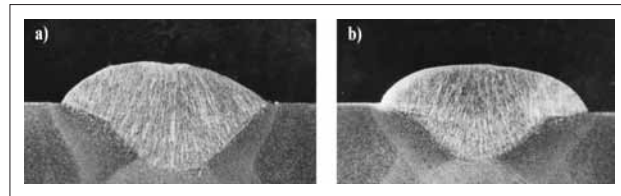


Figure 6 (a and b) Macro photos of series III weldments, segments 7 and 10, etched in Nital

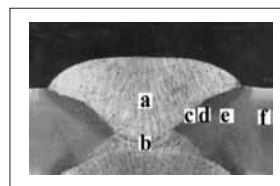


Figure 7 Macro photo of welded joint (segment 7, serie III) and locations of microstructural observations, etched in Nital

austenitic grains, and acicular ferrite (AF) inside the grains can be seen too [8]. Micro photo, Figure 8b presents the point of penetration between inner and outer welds. The influence of the second (outer) weld to the first one is clearly seen on the image. In the upper part of the picture, microstructure is dendritic, but in the lower part it can be seen that dendritic microstructure is partially destroyed as a result of a heat input of the second weld. Reaustenitisation contribute to the formation of equiaxed grains as seen in coarse grained HAZ. Microstructure in Figure 8c shows the coarse grained HAZ. It consists of coarse, equiaxed grains of primary austenite formed as result of retransformation. Proeutectoid ferrite and Widmanstatten ferrite are formed on the boundary of primary austenitic grains (black arrows) [9, 10]. Micro constituent found inside the grains is identified to be acicular ferrite. Point 8d represent fine grained normalized HAZ which generally poses very good mechanical properties, strength and impact toughness [9]. Figure 8e presents intercritically HAZ i.e. zone of partially transformation of perlite where max. temperature is between A_1 and A_3 points. Figure 8f shows microstructure of base material X52 with very fine grains (9-10 according to ASTM), which was not exposed to the influence of the welding thermal cycle.

Furthermore Charpy impact testing was performed with the notch located in different areas (weld metal, heat affected zone and base metal) followed by fractographic analyses. Fractographic analyses of the fractured surfaces (segment 7 serie III are presented in Figure 9. Figure 9a shows that base material has a ductile (dimple) type of fracture.

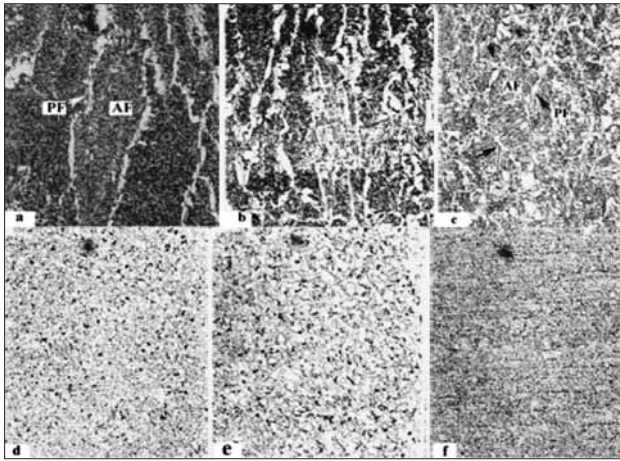


Figure 8 Microstructure of the locations presented on Figure 7, a. weld metal, b. penetration between the welds, c. CGHAZ, d. FGHAZ, e. ICHAZ, f. base metal fine grained microstructure, magnification x200, etched in Nital

The weld metal shows mixed type of fracture, containing both areas of brittle and ductile fracture (see Figure 9b). It was observed that the micro crack found in this region is parallel to the proeutectoid ferrite, marked with black arrow.

Testing of mechanical properties was performed according to GOST 20295 [7]. These investigations concerns segments 7-11 from Series III. Generally the following values are obtained $R_e = 389-403 \text{ N/mm}^2$, $R_m = 519-531 \text{ N/mm}^2$, $A_5 = 27-31\%$ and $KU = 106-125 \text{ J}$, at -40°C . Hardness measurements (Vickers method) were performed on the cross section containing base metal and weld joint. The measurements were defined in a way to investigate all characteristic zones of welded joint. In summary, it can be said that the lowest hardness values were recorded in the base metal (145-160 HV) because of the low carbon content, while the highest values were found in the weld metal ($\sim 200 \text{ HV}$). It should be noted that increase in hardness in the HAZ was not recorded. Generally, the highest measured value is 202 HV, which is much lower than 300 HV that is treated as a critical value for this type of steels [10].

CONCLUSIONS

Experiments showed that increase of the welding current improved penetration. Increasing of arc voltage resulted in a broadening of the weld face without a significant influence to the penetration, while the increasing of the welding speed lowers the welds. The best

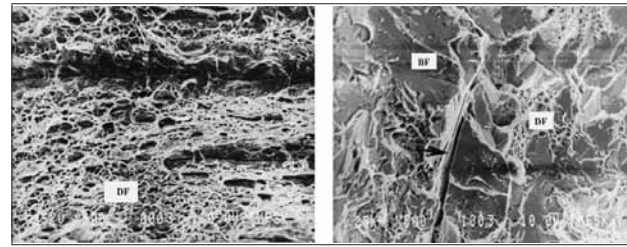


Figure 9 Fractured surface (segment 7 Serie III), a. base metal, b. weld metal

properties were found in the sample 7 (Series III) welded with the following parameters: wire I welding current 680 A, arc voltage 32 V. Wire 2 welding current 580 A, arc voltage 40 V. Welding speed is 1,4 m/min. Torches inclination: 90° for the first and 60° for the second wire.

Performed welding with self made equipment (serie II) didn't satisfy requirements. Pure welds quality and bed geometry was obtained. So improving weld properties and geometry, using this equipment will be the main target in our next investigation.

REFERENCES

- [1] American Petroleum Institute: Recommended pipeline maintenance welding practices. API RP 1107, USA.
- [2] G. Tither and W. E. Lauprecht, Pearlite-reduced HSLA steels for line pipe, *Metal Science and Heat Treatment*, December 07, 2004.
- [3] V. N. Marchenko and B. F. Zin'ko, Current trends in the development and production of steels and pipes for gas and oil pipelines; Translated from *Metallurg*, (2008) 3, 49-55.
- [4] American Petroleum Institute: API 5L standard
- [5] Lincoln Electric, *Welding Handbook*
- [6] Linde ELLIRA handbook, 1988.
- [7] Standard GOST 20295/85
- [8] G. M: Evans, N Bailey, *Metallurgy of Basic Weld Metal*; Abington Publishing, TWI, Cambridge England 1997.
- [9] Norman Bailey, *Weldability of Ferritic Steels*, Abington Publishing, TWI, Cambridge, England 1994.
- [10] S. Shanmugam, R.D.K. Misra, J. Hartmann and S.G. Jansto, Microstructure of high strength niobium-containing pipeline steel, *Materials Science and Engineering*, 441(2006) 1-2, 215-229.

ACKNOWLEDGMENT - The part of this study was conducted under support of Ministry of Science and Technological Development, Republic of Serbia

Note: English language lecturer: Biljana Mostrova, Faculty of Technology and Metallurgy, Skopje.